Applied Physics Letters

RESEARCH ARTICLE | DECEMBER 11 2023

An embedded microfluidic valve for dynamic control of cellular communication

Mark A. DeAngelis ; Warren C. Ruder ; Philip R. LeDuc

Appl. Phys. Lett. 123, 244103 (2023)
https://doi.org/10.1063/5.0172538

AIP Publishing

Applied Physics Letters ARTICLE pubs.aip.org/aip/apl

An embedded microfluidic valve for dynamic control of cellular communication

Cite as: Appl. Phys. Lett. **123**, 244103 (2023); doi: 10.1063/5.0172538
Submitted: 16 August 2023 · Accepted: 22 November 2023 ·
Published Online: 11 December 2023

Mark A. DeAngelis,[1] Warren C. Ruder,[1,2,3,4,a)] and Philip R. LeDuc[1,4,5,6,7,8,a)]

AFFILIATIONS

[1]Department of Mechanical Engineering, Carnegie Mellon University, Pittsburgh, Pennsylvania 15213, USA
[2]Department of Bioengineering, University of Pittsburgh, Pittsburgh, Pennsylvania 15219, USA
[3]Department of Pathology, University of Pittsburgh, Pittsburgh, Pennsylvania 15261, USA
[4]McGowan Institute for Regenerative Medicine, University of Pittsburgh, Pittsburgh, Pennsylvania 15219, USA
[5]Department of Biological Sciences, Carnegie Mellon University, Pittsburgh, Pennsylvania 15213, USA
[6]Department of Computational Biology, Carnegie Mellon University, Pittsburgh, Pennsylvania 15213, USA
[7]Department of Biomedical Engineering, Carnegie Mellon University, Pittsburgh, Pennsylvania 15213, USA
[8]Department of Electrical and Computer Engineering, Carnegie Mellon University, Pittsburgh, Pennsylvania 15213, USA

[a)]**Authors to whom correspondence should be addressed:** warrenr@pitt.edu and prl@andrew.cmu.edu

ABSTRACT

The communication between different cell populations is an important aspect of many natural phenomena that can be studied with microfluidics. Using microfluidic valves, these complex interactions can be studied with a higher level of control by placing a valve between physically separated populations. However, most current valve designs do not display the properties necessary for this type of system, such as providing variable flow rate when embedded inside a microfluidic device. While some valves have been shown to have such tunable behavior, they have not been used for dynamic, real-time outputs. We present an electric solenoid valve that can be fabricated completely outside of a cleanroom and placed into any microfluidic device to offer control of dynamic fluid flow rates and profiles. After characterizing the behavior of this valve under controlled test conditions, we developed a regression model to determine the required input electrical signal to provide the solenoid the ability to create a desired flow profile. With this model, we demonstrated that the valve could be controlled to replicate a desired, time-varying pattern for the interface position of a co-laminar fluid stream. Our approach can be performed by other investigators with their microfluidic devices to produce predictable, dynamic fluidic behavior. In addition to modulating fluid flows, this work will be impactful for controlling cellular communication between distinct populations or even chemical reactions occurring in microfluidic channels.

Cellular communication is a ubiquitous process that plays a key role in phenomena such as the contraction of muscle through coordinated cell actions,[1] the ability of plants to sense herbivores and pathogens,[2] and even the impact of the gut-microbiome on the proliferation of cancer cells.[3] One approach to exploring this interaction is through controlling the chemical environment with microfluidic systems.[4] While microfluidic devices with little to no direct fluid control have been used for many years to answer questions in the biomedical field with high efficiency and throughput,[5–8] more advanced fluid handling abilities may allow for more complex problems to be investigated. For instance, to control cellular communication, dynamic behavior in microfluidic devices can be implemented through a set of valves that control fluids. To achieve this, these valves would need to have several characteristics. First, the valve must be embeddable since cell–cell interactions would occur within the same microfluidic chip. This valve would also need to be tunable—or adjustable along a continuous range—so the amount of interaction between different cells can be manipulated, and dynamically controllable to allow for precise changes at specific moments in time. External pumps have been used to provide such control to microfluidic devices, and moving that capability to inside the device would enable more intricate fluid handling.[9–13] Next, automated (i.e., computer-based controlled) valves would allow for more repeatable actuation and remove the need for human intervention. Finally, using a single valve to implement fluid flow would allow the interaction between different types of cells to occur without forced flow, which could generate shear stress on the cells and lead to changes in signaling behavior or even apoptosis.[14]

TABLE I. Comparison of various valve designs based on their benefits and drawbacks for controlling cellular communication. The solenoid valve design used in this work to dynamically control fluid behavior was chosen due to its facile construction and ease of implementation using a microcontroller.

Design	Benefits	Drawbacks
Quake[15–17]	• Tunable • Small footprint ($100 \times 100\ \mu m^2$)	• Large, offboard pneumatic equipment • Short channels (10 μm) with small tunable flow range • Semicircular channels may make imaging difficult • Cleanroom fabrication required
Thermally actuated[18]	• Tunable • Small footprint (approx. $1\ mm^2$) • Easily controlled with a microcontroller	• Slower actuation times (>2 s) • Full closure of a channel takes > 30 s
Braille pins[19]	• Directly computer controllable • Simpler fabrication methods	• Not tunable with a single valve • Semicircular channels • Short channels (30 μm)
Solenoid[20]	• Tunable • Easily controlled with a microcontroller • Simpler fabrication methods • Up to 100 μm tall channels	• Solenoid adds significant height to device (approx. 3 cm) • Large footprint ($1 \times 1\ cm^2$)

There are currently many different microfluidic valve designs used in practice, each with its own characteristics, and a selected set are listed for comparison in Table I. One of the most common microfluidic valves, the Quake valve, allows for tunable flow by using pneumatic control channels powered by an external air supply and operates on a flow channel that is typically 10–30 μm tall, thus allowing for lower flow rates.[15–17] Thermally actuated valves employ a different design that uses a wire to heat up a medium that expands into a channel and tunably controls fluid flow. This can be easily operated with a microcontroller, and it can take as little as 2 s to completely close the channel.[18] Another computer-controlled valve uses braille pin arrays to press directly onto a channel and stop the fluid flow. With the use of multiple valves in series, tunable flow can be implemented through peristaltic action, since independent valves can only be used for open/closed behavior.[19] Finally, a solenoid valve designed by Hulme *et al.*[20] uses an electric solenoid that applies a force directly on top of a channel that is proportional to the voltage supplied to it. However, these valves have not been utilized to implement varying flow rates through microfluidic channels by modulating the input signal provided to them.

We report a tunable, embedded microfluidic valve that can control flow inside a device and use it to show dynamic behavior with a single valve. This work utilizes a solenoid valve constructed of low-cost components and is controlled with an Arduino microcontroller to vary flow rates and fluid profiles. We show that a desired fluidic behavior can be accurately produced by applying a time-varying voltage calculated from a model developed from experimental data. Utilizing our approach, investigators can implement the same valve in any microfluidic device and optimize fluid behavior for a specific application. Given that these valves are manufactured completely outside of a cleanroom utilizing 3D printed microfluidic molds replacing traditional photolithography techniques,[21–23] this method will allow researchers without access to a cleanroom to study dynamic microfluidic environments. Here, we present the fabrication of these valves, characterize their behavior, and demonstrate a control scheme to create a specific time-varying fluid profile. We used this control scheme to modulate the interface position between co-laminar fluid streams, which previously has been used to investigate spatiotemporal cellular dynamics.[10,24]

The fully functioning microfluidic device was created in two stages. First, taking inspiration from Hulme *et al.*,[20] a solenoid valve was fabricated by bonding a polydimethylsiloxane (PDMS) membrane to a PDMS nut [Fig. 1(a)]. We made this nut by pouring PDMS around a bolt to cast the thread pattern and allow for an electric solenoid to be screwed into it. Additionally, a hole was punched into the center of the membrane of the valve so it could be aligned to a channel during the next stage. Second, this valve was embedded into a microfluidic device. Initially, a spin-coated layer of PDMS was partially cured on a silicon wafer with the desired channels and acted as a barrier between the valve and the microfluidic channel. Then, a valve was placed above a channel and additional PDMS was poured around the valve to make the finished device [Figs. 1(a) and 1(b)]. The spin-coated layer was only partially cured for two reasons: to prevent the valve from drifting in position as the PDMS poured around it cures and to prevent air bubbles from becoming trapped under the valve. Furthermore, to ensure full bonding of the different PDMS layers, the PDMS in the spin-coated layer was mixed at a lower curing agent to elastomer base ratio (1:15) so there would be diffusion of the curing agent between layers and enhance cross-linking at the interface.

For the experiments we conducted to test these solenoid valves, we used a 60 μm tall Y-channel geometry. This design had two 50 μm wide inlets, a 100 μm wide outlet, and a scale with 100 μm increments that started at the intersection of the two inlets to provide measurements along the outlet channel. Additionally, markers were placed at 1 mm increments along both inlets to aid in aligning the prefabricated valve 2 mm away from the outlet. By using this Y-channel design with fluid moving in the laminar flow regime, two distinct, adjacent (i.e., coflowing) fluid streams were visible in the outlet channel since the inlet streams did not convectively mix, given the laminar flow regime. To view these separate fluid streams, each inlet contained either clear or red-dyed distilled water. As shown in Figs. 2(a) and 2(b), the solenoid valve was placed on the inlet channel with red-dyed water. Thus, by changing the voltage applied to the solenoid through an Arduino,

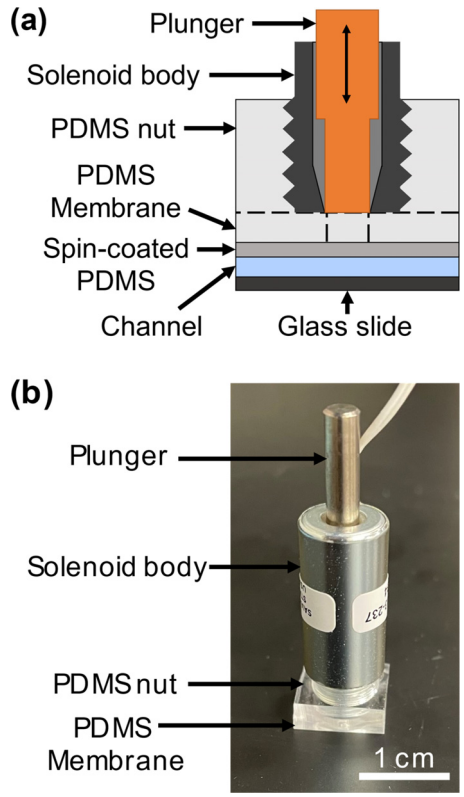

FIG. 1. Solenoid valve construction and resulting system. (a) An embedded valve consists of several PDMS layers, including a nut and membrane, before being placed on top of a spin-coated PDMS layer above the desired channel. (b) An electric solenoid screwed into the fabricated valve can be used in any microfluidic device since the valve is made before the device is fabricated.

the width of the red fluid stream in the outlet would change [Fig. 2(c)]. This occurs because the force generated by the solenoid decreases the cross-sectional area of the channel and reduces the flow rate. A full derivation of this behavior can be found in the supplemental materials.

The width of this red water stream, and thus the interface position, was measured for a range of applied voltages to the solenoid to characterize the behavior of the valve in this microfluidic device. For each applied voltage, the average width was calculated with a custom Python script that identified the region of an image that was red water and then counted the number of pixels that fell on a vertical line 100 μm away from the intersection of the Y-channel device [Fig. 3(a)]. As shown in the characterization curve shown in Fig. 3(b), the tunable region of the valve was from 0 to 20 V. The data from this range of the characterization curve was then plotted on an inverted graph—where the independent variable was the normalized width rather than voltage. To determine the required voltage to create a specific flow profile for the red water stream, a regression model was developed using these data and had an R^2 of 0.959 [Fig. 3(c)].

To show that the solenoid valve can be used to create a specific, dynamic fluid profile, we used our regression model to determine the required voltage input to drive the interface position of the co-laminar fluid stream in a sinusoidal pattern with a period of 5 s [Fig. 4(a)]. Applying this voltage to the solenoid valve resulted in a measured fluid profile that resembled a sinusoid [Fig. 3(b)]. However, the measured output had a phase shift with respect to the desired sinusoidal profile. By fitting a sinusoidal function to these data, the curve fit had an R^2 value of 0.985, showing that much of the variance in the measured fluid profile was explained by a sinusoid [Fig. 3(c)]. Additionally, this curve fit revealed that the output had a period of 5.115 s, giving a percent error of 2.29% on the period, and a phase shift of 574 ms. This phase shift was partially due to a delay between beginning the video capture and starting the Arduino to control the valve and could be reduced through code optimization. Overall, these results indicate that the valve can be used to accurately create specific flow profiles within a microfluidic device.

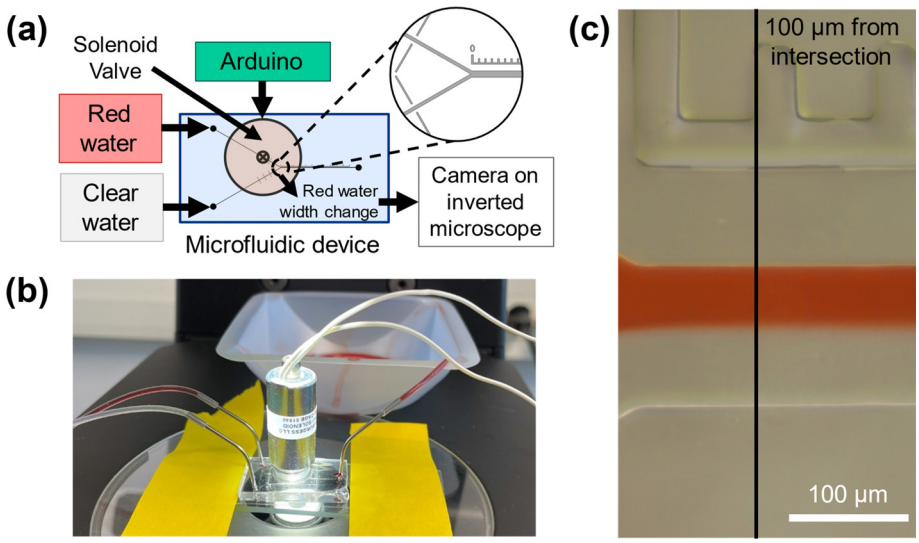

FIG. 2. Measuring the fluid profile enabled by our solenoid based approach. (a) Schematic of the microfluidic setup. The solenoid valve is operated by an Arduino and controls the flow of the red-dyed water. This changes the width of the fluid stream in the outlet channel, which is measured on an inverted optical microscope. (b) An image of the microfluidic device in use. Red and clear water enter the device through tubing connected to syringe needles on the left side. The solenoid is powered through the two white wires exiting the top of its body. (c) An image of the outlet channel that indicates the point where the width of the red water was measured using the scale bar included in the microfluidic device.

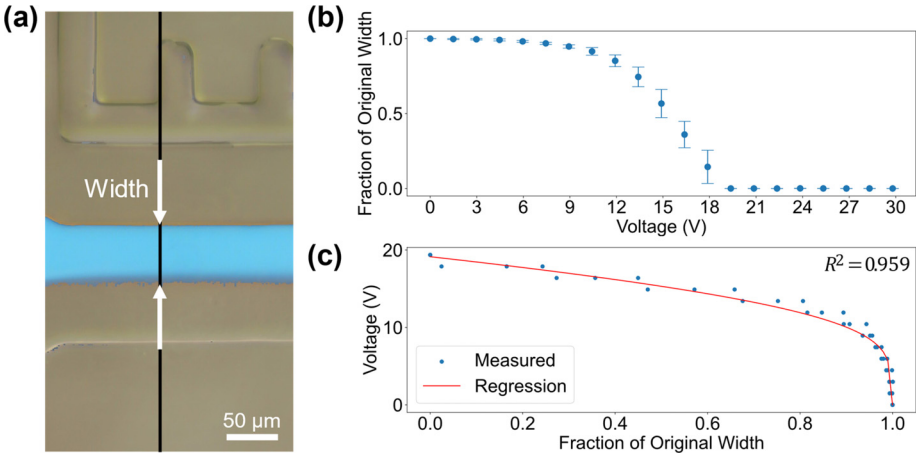

FIG. 3. Results of the valve characterization process relative to the width of the stream. (a) Using the OpenCV library in Python, the red water region was identified (highlighted in blue), and the width of the fluid stream was measured by counting the number of pixels that lie on a vertical line 100 μm away from the inlet intersection. (b) The normalized width of the red water steam in the outlet channel when the solenoid valve was powered with 0–30 V. Points represent the mean of three tests with error bars of one standard deviation. (c) A ridge regression model was developed using the characterization data from (b) to identify the required voltage to obtain a specific width.

In order to test the capabilities of our system, we actuated the solenoid with a range of input signal frequencies varying over three orders of magnitude [Fig. 5(a)]. First, for a given target frequency, we determined the voltage input necessary to generate a sinusoidal fluid output profile and applied it to the solenoid. After recording the position of the interface in the device, we applied a fast Fourier transform (FFT) to this measured output data, which revealed the dominant frequency in the physical behavior of the system [Fig. 5(b)]. As shown in Fig. 5(c), by taking the inverse FFT of frequency responses that only included the dominant frequency and 0 Hz offset, the identified sinusoid could be compared to the measured response through the coefficient of determination, R^2 (see the supplementary material for full details). When performing this process for triplicate experiments from 0.005 to 5 Hz, frequencies below 1 Hz had R^2 values above 80%. The drop in R^2 observed for frequencies above 1 Hz meets expectations, given that fewer points are collected per cycle of a higher frequency sinusoid when using a fixed sampling rate, so small errors in measurement are more likely to impact the result.

We have shown a microfluidic valve that can dynamically control fluid flow behavior inside a microfluidic device. After characterizing the valve for a Y-channel microfluidic geometry, a sinusoidal output flow profile was accurately created. This demonstrates how a single embedded valve can be controlled to produce dynamic fluidic behavior. The solenoid valve we used has several added benefits for this application. First, this valve offers researchers who have limited resources the ability to dynamically control microfluidic environments since they can be constructed completely outside of a cleanroom. This includes spin coating a thin layer of PDMS on the microfluidic wafer, as low-cost spin coaters can be built in the lab for as low as $30.[25] Second, since the primary active component of these valves—the electric solenoid—can be easily removed from a device, the most expensive component of an individual valve can be reused across several microfluidic chips. If a single microfluidic device is only used one time, this solenoid valve provides significant time and cost savings because of its simple fabrication and reusability. Finally, given that these valves are electrically powered rather than pneumatically, they can be controlled without additional external equipment such as pumps or lab air supplies. It is important to note that these valves are most applicable to microfluidic devices that are (1) made with elastomers, (2) do not have multiple fluidic channels within the 1 cm^2 area of the valve, and (3) do not contain electrical components or magnetic fluids that could be sensitive to the actuation of the solenoid. Yet, given that the approach we have presented for controlling the solenoid valve relies only on the data collected from the fluidic system, it could be applied to other types of microfluidic valves that meet user requirements.

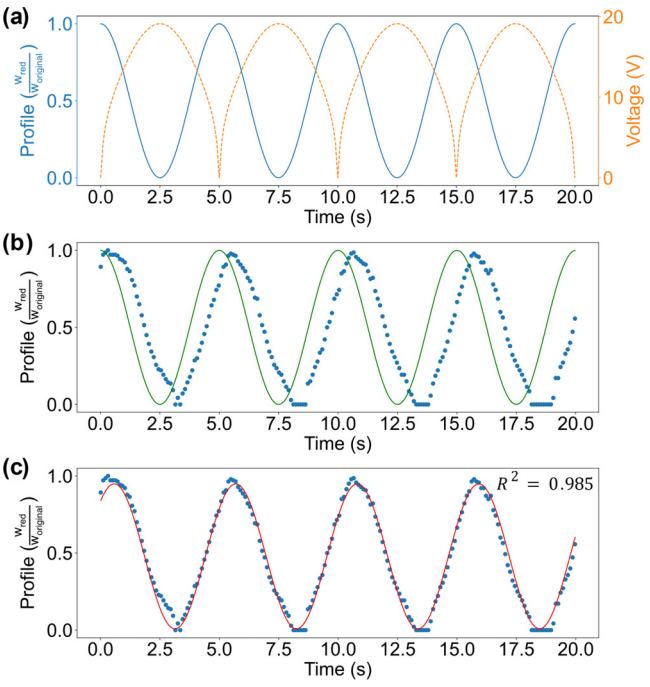

FIG. 4. Driving the interface position of a co-laminar fluid stream in a sinusoidal profile with the solenoid valve. The profile on the vertical axis for all plots indicates the ratio of the width of the current red water stream to its original width when the solenoid valve is not powered. (a) To create a sinusoidal output, the regression model was used to calculate the required voltage waveform to apply to the valve. (b) A phase shift was observed between the expected forced output (green line) and the measured result (blue dots). (c) A cosine wave (red line) was fit to the measured fluid profile (blue dots) and showed high agreeability.

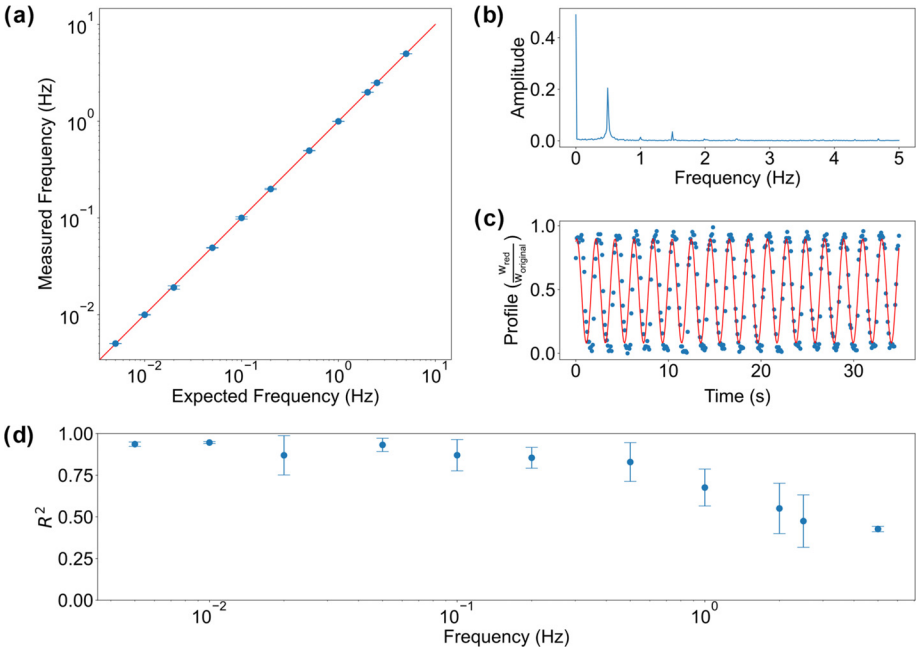

FIG. 5. Frequency performance characterization for the solenoid valve. (a) The range for the frequency of actuation was determined by identifying the dominant frequency of a FFT performed on the measured data. Over three orders of magnitude, the valve was able to reproduce an output with the same frequency as desired. (b) An example of the results from the FFT for one test of 0.5 Hz, where the dominant frequency was identified as the peak at 0.493 Hz. (c) Using the inverse FFT for the dominant frequency and 0 Hz offset terms, a single sinusoid was compared to the measured data. This plot shows the results for the same test from (b). (d) The R^2 of the inverse FFT to the measured data for all tested frequencies. Points represent the mean of three tests with error bars of one standard deviation for both (a) and (d).

While we showed this valve working in a specific microfluidic device, our approach can be extrapolated to other channel geometries. After embedding a valve into a microfluidic device, the system can be characterized with dyed fluid so an input–output relationship can be determined with the electrical input to the valve and camera data output. Here, this output was the width of a red-dyed water stream in the outlet of our device, but it could be the diameter of a droplet for water-in-oil droplet applications[23,26,27] or the color of a mixed solution of multiple, dyed fluidic inputs. In any case, this characterized relationship can be utilized to develop a model to calculate the required input for a specific behavior. Once this model is created, a microfluidic system employing fluids of any color, including clear fluids, could be accurately controlled. This is particularly important for cell culture experiments where the color of reagents is fixed. As a result, researchers will be able to more easily study and control complex biological systems or mass transport effects with this methodology and the unique advantages offered by these solenoid valves.

See the supplementary material for details on the microfluidic device fabrication process, the control setup, and system characterization.

This work was supported by awards from the Air Force Office of Scientific Research (No. FA9550-18-1-0262), the NIH Director's New Innovator Award (No. DP2-GM132934), the National Institute of Health (No. R21AR08105201A1; No. R01AG06100501A1), the National Science Foundation (No. CMMI-1946456), and the Biomechanics in Regenerative Medicine Training Program (No. NIH-NIBIB T32-EB034216). Any opinions, findings, and conclusions or recommendations expressed in this material are those of the authors and do not necessarily reflect the views of the National Science Foundation. The authors also thank H.C. Fuller and U.M. Sönmez for insightful discussions on microfluidics.

AUTHOR DECLARATIONS

Conflict of Interest

The authors have no conflicts to disclose.

Author Contributions

Mark Anthony DeAngelis: Conceptualization (equal); Formal analysis (equal); Investigation (equal); Methodology (equal); Software (equal); Visualization (equal); Writing – original draft (equal). **Warren Christopher Ruder:** Conceptualization (equal); Funding acquisition (equal); Methodology (equal); Resources (equal); Supervision (equal); Writing – review & editing (equal). **Philip R. LeDuc:** Conceptualization (equal); Funding acquisition (equal); Methodology (equal); Supervision (equal); Writing – review & editing (equal).

DATA AVAILABILITY

The data that support the findings of this study are available within the article and its supplementary material.

REFERENCES

[1]M. Kaya, Y. Tani, T. Washio, T. Hisada, and H. Higuchi, Nat. Commun. **8**(1), 16036 (2017).
[2]R. Karban, Annu. Rev. Ecol. Evol. Syst. **52**(1), 1–24 (2021).
[3]G. D. Sepich-Poore, L. Zitvogel, R. Straussman, J. Hasty, J. A. Wargo, and R. Knight, Science **371**(6536), eabc4552 (2021).
[4]Y. Sei, K. Justus, P. LeDuc, and Y. Kim, Microfluid. Nanofluid. **16**(5), 907 (2014).
[5]J. S. Jeon, S. Bersini, M. Gilardi, G. Dubini, J. L. Charest, M. Moretti, and R. D. Kamm, Proc. Natl. Acad. Sci. U. S. A. **112**(1), 214 (2015).

[6]A. Mathur, P. Loskill, K. Shao, N. Huebsch, S. Hong, S. G. Marcus, N. Marks, M. Mandegar, B. R. Conklin, L. P. Lee, and K. E. Healy, Sci. Rep. **5**(1), 8883 (2015).
[7]M. O. Din, T. Danino, A. Prindle, M. Skalak, J. Selimkhanov, K. Allen, E. Julio, E. Atolia, L. S. Tsimring, S. N. Bhatia, and J. Hasty, Nature **536**(7614), 81 (2016).
[8]E. Osmekhina, C. Jonkergouw, G. Schmidt, F. Jahangiri, V. Jokinen, S. Franssila, and M. B. Linder, Commun. Biol. **1**(1), 97 (2018).
[9]Y. Kim, B. Kuczenski, P. R. LeDuc, and W. C. Messner, Lab Chip **9**(17), 2603 (2009).
[10]B. Kuczenski, W. C. Ruder, W. C. Messner, and P. R. LeDuc, PLoS One **4**(3), e4847 (2009).
[11]Y. Kim, M. Hazar, D. S. Vijayraghavan, J. Song, T. R. Jackson, S. D. Joshi, W. C. Messner, L. A. Davidson, and P. R. LeDuc, Proc. Natl. Acad. Sci. U. S. A. **111**(40), 14366 (2014).
[12]J. R. Lake, K. C. Heyde, and W. C. Ruder, PLoS One **12**(4), e0175089 (2017).
[13]M. R. Behrens, H. C. Fuller, E. R. Swist, J. Wu, M. M. Islam, Z. Long, W. C. Ruder, and R. Steward, Sci. Rep. **10**(1), 1543 (2020).
[14]D. Huber, A. Oskooei, X. Casadevall i Solvas, A. deMello, and G. V. Kaigala, Chem. Rev. **118**(4), 2042 (2018).
[15]M. A. Unger, H.-P. Chou, T. Thorsen, A. Scherer, and S. R. Quake, Science **288**(5463), 113 (2000).
[16]D. Gray-Scherr, H. Gasvoda, A. Hadsell, L. Miller, E. Demir, and I. E. Araci, J. Micromech. Microeng. **32**(12), 125002 (2022).
[17]B. Che, D. Sun, N. Yan, W. Zhao, Y. Liu, G. Jing, and C. Zhang, Adv. Intell. Syst. **5**(5), 2200366 (2023).
[18]M. Sesen and C. J. Rowlands, Microsyst. Nanoeng. **7**(1), 48 (2021).
[19]W. Gu, X. Zhu, N. Futai, B. S. Cho, and S. Takayama, Proc. Natl. Acad. Sci. U. S. A. **101**(45), 15861 (2004).
[20]S. E. Hulme, S. S. Shevkoplyas, and G. M. Whitesides, Lab Chip **9**(1), 79 (2009).
[21]N. Bhattacharjee, A. Urrios, S. Kang, and A. Folch, Lab Chip **16**(10), 1720 (2016).
[22]M. de Almeida Monteiro Melo Ferraz, J. B. Nagashima, B. Venzac, S. Le Gac, and N. Songsasen, Sci. Rep. **10**(1), 994 (2020).
[23]T. D. Anyaduba, J. A. Otoo, and T. S. Schlappi, Micromachines **13**(11), 1946 (2022).
[24]S. Takayama, E. Ostuni, P. LeDuc, K. Naruse, D. E. Ingber, and G. M. Whitesides, Nature **411**(6841), 1016 (2001).
[25]M. Sadegh-cheri, J. Chem. Educ. **96**(6), 1268 (2019).
[26]S.-Y. Teh, R. Lin, L.-H. Hung, and A. P. Lee, Lab Chip **8**(2), 198 (2008).
[27]Y. Zhou, Z. Yu, M. Wu, Y. Lan, C. Jia, and J. Zhao, Talanta **253**, 124044 (2023).